Analyst

Extension of the broadband single-mode integrated optical waveguide technique to the ultraviolet spectral region and its applications

Rodrigo S. Wiederkehr† and Sergio B. Mendes*

We report here the fabrication, characterization, and application of a single-mode integrated optical waveguide (IOW) spectrometer capable of acquiring optical absorbance spectra of surface-immobilized molecules in the visible and ultraviolet spectral region down to 315 nm. The UV-extension of the single-mode IOW technique to shorter wavelengths was made possible by our development of a low-loss single-mode dielectric waveguide in the UV region based on an alumina film grown by atomic layer deposition (ALD) over a high quality fused silica substrate, and by our design/fabrication of a broadband waveguide coupler formed by an integrated diffraction grating combined with a highly anamorphic optical beam of large numerical aperture. As an application of the developed technology, we report here the surface adsorption process of bacteriochlorophyll *a* on different interfaces using its Soret absorption band centred at 370 nm. The effects of different chemical compositions at the solid–liquid interface on the adsorption and spectral properties of bacteriochlorophyll *a* were determined from the polarized UV-Vis IOW spectra acquired with the developed instrumentation. The spectral extension of the single-mode IOW technique into the ultraviolet region is an important advance as it enables extremely sensitive studies in key characteristics of surface molecular processes (*e.g.*, protein unfolding and solvation of aromatic amino-acid groups under surface binding) whose spectral features are mainly located at wavelengths below the visible spectrum.

Introduction

Molecular adsorption and interactions at surfaces is a topic of increasing interest in many theoretical and experimental studies due to its importance in many applications such as in biosensors,[1] biomaterials for implants,[2,3] tissue engineering,[4,5] and chromatography.[6,7] There are currently several excellent probing techniques in use to quantify molecular adsorption[8–11] at the monolayer and sub-monolayer levels. Ellipsometry obtains the refractive index and surface coverage of a molecular adsorbate by measuring changes in the two ellipsometric angles of polarized reflected light.[3,12] Surface plasmon resonance measures the coupling angle that a particular laser line generates a plasmon wave on a noble metal film; such a coupling angle is highly sensitive to the presence of an analyte on the metal–liquid interface.[1,13] Optical waveguide light-mode spectroscopy is based on grating-assisted coupling of a particular laser frequency into a guiding layer; the adsorbed molecular density and refractive index are obtained by measuring changes in the coupling angles

as they are very sensitive to the presence of adsorbates on the surface of the guiding layer.[3,14] Scanning angle reflectometry obtains the thickness and refractive index changes on a solid–liquid interface due to molecular adsorption by measuring the changes in the polarized reflected light around the Brewster angle.[15,16] A quartz microbalance measures the adsorbed mass by detecting changes in the resonant frequency of a piezoelectric crystal excited by an external electric field.[17,18] However, an important limitation in those techniques has been the inability (or difficulty) to provide broadband optical spectroscopic information. Such spectroscopic information can potentially be quite useful to address possible conformational and structural changes of the adsorbed molecules due to their interaction with different chemical environments on the surface of interest.

Broadband attenuated total reflectance measurements based on a 30 μm thick internal reflection element (*i.e.*, a multi-mode waveguide) have been successfully demonstrated.[19,20] Such confinement of the light beam provides a sensitivity enhancement of about two orders of magnitude (300×–400×) compared to measurements in direct transmission or single-bounce reflection to probe surface-adsorbed chromophores. By reducing the thickness of the internal reflection element, both the number of bounces (per unit length of beam propagation inside the guide) and the sensitivity of the device increase. When such reduction is taken to its absolute minimum size (below which the

Department of Physics and Astronomy, University of Louisville, Louisville 40292, Kentucky, USA. E-mail: sb.mendes@louisville.edu; Fax: +1 (502) 852-8128; Tel: +1 (502) 852-0908

† Current address: IMEC – Interuniversity Microelectronics Center, Life Science and Technologies Department, Kapeldref, 75, 3001 Leuven, Belgium.

light beam would no longer be guided inside the internal reflection element), one obtains a single-mode integrated optical waveguide (IOW) with the ultimate sensitivity enhancement, which is typically more than 4 orders of magnitude compared to measurements in direct transmission or single-bounce reflection to probe surface-adsorbed chromophores (approximately 52 000× in this work with an IOW thickness of 0.178 μm). The single-mode IOW is a highly sensitive technique to investigate surface adsorbed molecules due to the long and strong optical interaction of the evanescent field of a propagating guided mode.[21–29] The combination of the IOW technique with broadband couplers has enabled optical spectroscopic studies of sub-monolayer assemblies.[30–32] Polarized absorbance data obtained with a single-mode IOW spectrometer can be directly related to the surface concentration and molar absorptivity of the adsorbed molecular layer under investigation.[33] The single-mode broadband IOW technique has already been shown to be very effective in studying molecular adsorbates from absorbance measurements in the visible region of the spectra.[30–32,34,35] However, none of the studies presented in the literature using the single-mode IOW platform has been able to acquire spectroscopic data of adsorbed chromophores below 400 nm. And this has been an important limitation since several chromophores relevant to studies of biological materials[36–39] have their absorption transition bands located in the ultraviolet spectral region. In this report we describe the development of a single-mode broadband integrated optical waveguide technique in the ultraviolet spectral region and provide initial applications to demonstrate its performance. To attest the instrument capability in the ultraviolet region, the Soret band of bacteriochlorophyll *a* centred at 370 nm was measured. Waveguide samples were functionalized either with a hydrophilic or a hydrophobic monolayer to allow investigations of surface adsorption of bacteriochlorophyll *a* onto different surface environments.

Experimental procedures

Ultraviolet integrated optical waveguide spectrometer

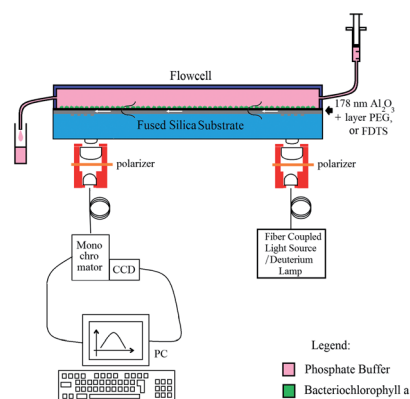The overall setup of the IOW spectrometer is shown in Fig. 1 and the essential components of the instrument comprises a single-mode planar optical waveguide with a pair of integrated grating couplers, optical components for shaping the in-coupling and out-coupling light beams, a monochromator, an UV broadband light source, a charge coupled device (CCD) array detector, and a flowcell.

Due to its high transparency in the near ultraviolet (and visible) region, an alumina thin-film was employed as a single-mode optical waveguide, which was grown on top of a high quality fused silica substrate (Plan Optik AG, Germany) with a roughness better than 0.5 nm. The alumina thin film was coated on the silica substrate using an atomic layer deposition tool (Beneq TFS200). The chemical precursors used for the ALD growth of the alumina film were tri-methyl-aluminum and water. Those precursors were alternatively injected inside the deposition chamber under vacuum to create a self-limiting monolayer for each cycle.[40] The deposition temperature in the reaction chamber was set at 250 °C, and 1690 cycles were required to reach the target thickness of approximately 178 nm. The ALD process was chosen due to its ability to deliver very low-loss optical waveguides in the ultraviolet region (less than 5 dB cm^{-1} at 325 nm). Additional information on the ALD process and the full characterization of the alumina waveguide films have been described in detail elsewhere.[40]

The coupling of a light beam with a broad spectral content into and out of a single-mode waveguide was achieved by using integrated diffraction gratings in combination with highly anamorphic optical components, which include solid immersion cylindrical lenses to manage an optical beam of large numerical aperture. The approach was originally developed by us for the visible spectral region,[41] and here we highlight the relevant modifications to allow its extension to the UV region. Specifically, in this work we used a pair of surface-relief diffraction gratings on a fused silica substrate with a periodic modulation of 200 nm, which provides a coupling bandwidth of approximately 160 nm centred at a wavelength of 325 nm.

Those diffraction gratings (one for input and one for output coupling) were separated by 34 mm from each other. By using a holographic patterning technique based on a Lloyd mirror configuration,[42] the photoresist film (S1805) was exposed under the two-beam interference pattern of the 325 nm line of a He–Cd laser. Next, the holographically exposed samples were chemically developed by Shipley 351 solution to create a photopattern in the photoresist film. In order to transfer the periodic modulation created in the photopattern to the silica substrate surface, the sample was dry-etched using Ar and CF_4 as etchants.

The light source used for the spectroscopic experiments was a deuterium lamp (Hamamatsu UV-Vis fibre light source, L10290) with a strong spectral emission from 200 to 500 nm. An UV-compatible linear polarizer (BBO from Red Optronics, US) was placed in the optical path, as indicated in Fig. 1, to allow only for the transverse light mode (TE) to couple with the waveguide. The out-coupled light beam was collected and fiber-guided to a monochromator (SpectraPro 2300, Princeton Instruments) that dispersed the light beam to a CCD detector (Pixis 400, Princeton Instruments) where each column of the detector corresponds to a particular wavelength. On the top of

Fig. 1 Single-mode UV-IOW spectrometer created to acquire spectra of adsorbed molecules in the ultraviolet region.

the waveguide surface a flowcell was mounted to inject aqueous solutions. The total amount of liquid necessary to cover the whole waveguide surface is approximately 2 ml. All data acquisitions were performed at room temperature (25 °C). Fig. 2 describes the overall optical throughput of the device, which involves the lamp emission, the bandwidth of the diffraction grating couplers, waveguide attenuation losses, and the detector response.

Waveguide surface modification

The alumina waveguide surface was chemically modified by coating organic monolayers with different hydrophobicities using Molecular Vapor Deposition.[43] The peg silane hydrophilic monolayer was obtained by sequential injection of methoxy-(polyethyleneoxy)propyltrimethoxysilane (Gelest Inc.) and water on the reaction chamber under vacuum with a reaction time of 15 minutes. The FDTS hydrophobic monolayer was obtained by sequential injection of (heptadecafluoro-1,1,2,2-tetrahydrodecyl) trichlorosilane (Gelest Inc.) and water on the reaction chamber with a reaction time of 5 minutes.[44] In both cases the temperature of the precursors was kept constant at 55 °C and the MVD reaction chamber was at 35 °C. Prior to the MVD deposition, an oxygen plasma treatment was performed for 60 s to remove any organic residue from the alumina surface. To confirm the film properties the contact angle of a water droplet was measured for each coating. The results, which are presented in Fig. 3, were obtained using the software (called Dropsnake) developed by Stalder et al.[45] to obtain the contact angle by using active contours (B-spline traces) to shape the water drop. In addition, we noticed that the aluminum oxide layer, when compared to polymeric or metal surfaces, has improved stability and durability of the deposited peg silane and FDTS films most likely due to the higher density of reactive hydroxyl groups on the surface of the oxide film.[44]

Sample preparation

Bacteriochlorophyll *a* from *Rhodopseudomonas sphaeroides*, which is a photosynthetic pigment found in purple bacteria,

Fig. 3 Contact angle measurements for the different waveguide surfaces. The results confirm that FDTS is a hydrophobic layer and peg silane is a hydrophilic coating on top of the aluminum oxide layer.

was commercially obtained (Sigma Aldrich B5906) and dissolved in 10 ml of methanol (EMD Chemicals, MX0480-1 OmniSolv ≥ 99.9%). The concentration of bacteriochlorophyll *a* in solution was obtained by measuring the Q band (771 nm) absorbance peak with a conventional spectrophotometer (Cary 300, Varian Inc.) and using the molar absorptivity ($\varepsilon_{771} = 54\ 800$ M^{-1} cm^{-1}) of bacteriochlorophyll *a* dissolved in methanol, which is available in the literature.[46]

To ensure that the concentration of bacteriochlorophyll *a* does not suffer any alteration during the experiments the sample solution that went through the waveguide flowcell was collected and measured. Fig. 4 shows the absorbance spectra obtained for solutions with the same concentration of bacteriochlorophyll *a* but with different salt concentrations, [NaCl]. To obtain solutions with final concentrations of 0.125 μM and 0.0125 μM, the stock solution was dissolved in 7 mM sodium phosphate (NaH$_2$PO$_4$, pH at 7.2) with [NaCl] between 1 mM and 20 mM. As evidenced by the Soret absorbance peak centred at 370 nm shown in Fig. 4, the spectroscopic characteristics of bacteriochlorophyll *a* dissolved in phosphate buffer solution remains fairly constant regardless of the ionic strength.

The sensitivity factor, which is defined as the ratio between the absorbance measured using a waveguide platform A_{WG} and the absorbance measured in direct transmission A_{TR} (for an arbitrary layer of chromophores), is given by eqn (1):[33,47]
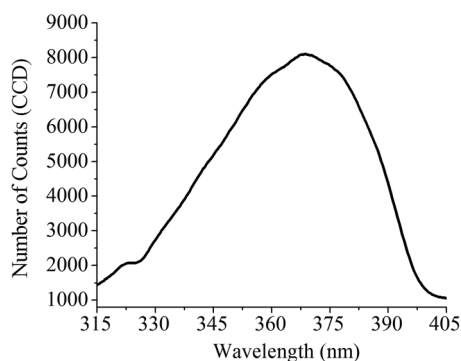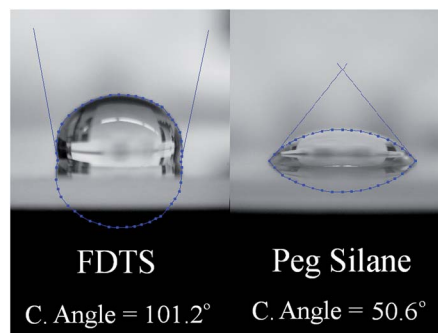

Fig. 2 Spectral bandwidth coupled to the single-mode UV-IOW spectrometer setup after mounting the flowcell and injecting phosphate buffer. The coupled spectral range did not change after functionalizing the waveguide surface with peg silane or FDTS monolayers.
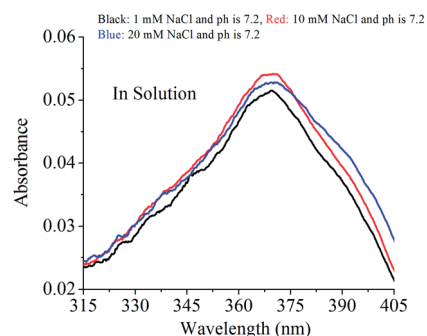

Fig. 4 Absorbance spectra measured for bacteriochlorophyll *a* dissolved in phosphate buffer solutions with different [NaCl].
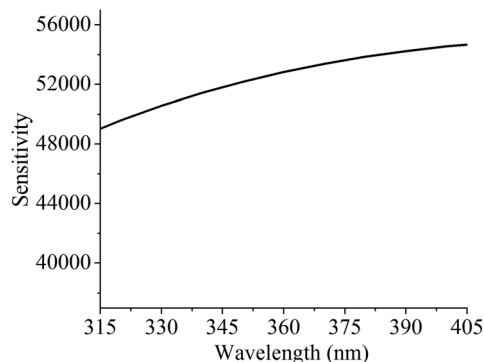
Fig. 5 Sensitivity factor calculated for the single-mode UV-IOW with 178 nm thickness and considering the following values for the constants: $L = 3.4$ cm, $n_c = 1.33$, with the approximation that $n_l \approx n_c$. The effective index, N_{TE}, and the effective thickness, $t_{eff,TE}$, were calculated from the waveguide dispersion equation. The refractive index of the alumina film was calculated using the relationship $n_w(\lambda) = a + b/\lambda^2 + c/\lambda^4$, where $a = 1.64576$, $b = 42.89898$, and $c = 308\,958\,233.142$ from ref. 40.

$$S = \frac{A_{WG}}{A_{TR}} = \frac{A_{WG}}{\varepsilon_{surf}\Gamma} \quad (1)$$

where ε_{surf} is the molar absorptivity of the surface bonded chromophores and Γ is the chromophore surface density. The sensitivity factor, which is a polarization-dependent factor, is given by eqn (2) for the TE polarized light:[47]

$$S_{TE} = \frac{2\,n_l\,\left(n_w^2 - n_{TE}^2\right)L}{N_{TE}\,\left(n_w^2 - n_c^2\right)t_{eff,TE}} \quad (2)$$

where n_l is the real part of the refractive index of the adsorbed analyte, n_w is the refractive index of the alumina waveguide, n_c is the refractive index of the buffer solution, N_{TE} is the effective index of the waveguide, $t_{eff,TE}$ is the effective thickness of the waveguide (which is related to the physical thickness t of the guiding film[47]), L is the distance between the input and output couplers. For the single-mode IOW used in this work the sensitivity factor is presented in Fig. 5 as a function of the wavelength for the spectral region of interest here. The extremely high sensitivity factor makes possible the investigation of low surface concentration of adsorbed species.

Results and discussion

Absorbance of the bacteriochlorophyll *a* sub-monolayer

The absorbance spectra recorded using the UV-IOW spectrometer for bacteriochlorophyll *a* adsorbed onto surfaces with different chemical compositions and from solutions with different ionic strengths are presented next. We show in Fig. 6 the data for the surface functionalized with a peg silane hydrophilic monolayer and in Fig. 7 with a FDTS hydrophobic layer.

All spectra were collected after the equilibrium had been reached between bacteriochlorophyll *a* species dissolved in solution and adsorbed onto the different surfaces that occurred after 35–40 minutes of incubation. This means no
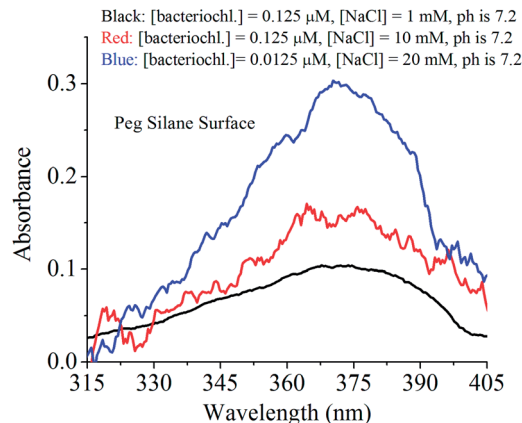

Fig. 6 Absorbance spectra for bacteriochlorophyll adsorbed onto hydrophilic surface. The increase on [NaCl] in dissolving solution from 1 mM to 20 mM raised the absorbance by a factor of 3 even with decrease of [bacteriochlorophyll] in solution by a factor of 10.
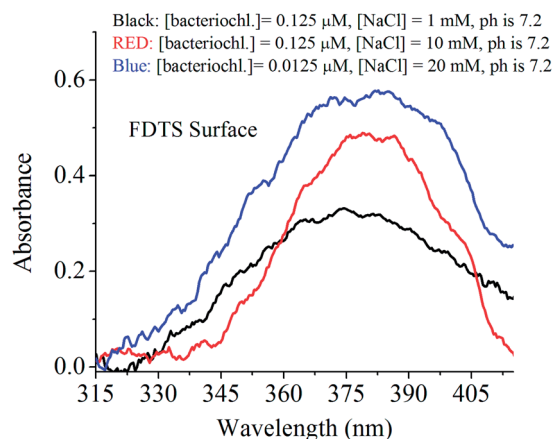

Fig. 7 Absorbance spectra for bacteriochlorophyll adsorbed onto hydrophobic surface. The absorbance increased by a factor of 2.4 when the [NaCl] in the dissolved solution was raised from 1 mM to 20 mM and the [bacteriochlorophyll] in solution decreased by a factor of 10.

more changes are observed on the absorbance spectra. After the incubation period the flow cell was flushed with pure DI water and the spectra were acquired again. This step is to ensure that the absorbance data acquired are really from the absorbed molecules, not from the solution. To avoid excessive surface adsorption (which would eliminate any output signal from the waveguide spectrometer) for solutions with 20 mM of [NaCl], the concentration of bacteriochlorophyll was reduced by 10 times (from 0.125 μM to 0.0125 μM) prior to adsorption onto the FDTS hydrophobic or peg silane hydrophilic surfaces.

Surface coverage of bacteriochlorophyll *a* adsorbed onto different surfaces

In order to calculate the surface density, eqn (1) was solved for Γ, which gave us:

$$\Gamma = \frac{A_{\text{WG,TE}}}{S_{\text{TE}}\varepsilon_{\text{surf}}} \qquad (3)$$

where we use the experimental results of the peak absorbance $A_{\text{WG,TE}}$ measured by the single-mode UV-IOW spectrometer and the sensitivity factor S_{TE} calculated from eqn (2).

The results for surface coverage adsorbed onto hydrophilic and hydrophobic layers from solutions with different ionic strengths are presented in Fig. 8. Our experimental results show that, regardless of the salt concentration, the surface coverage is consistently higher for the hydrophobic surface. Also, we observe that the surface concentration increased by 2.3 times for peg silane and 1.4 times for the FDTS surface when the [NaCl] in solution increased from 1 mM to 20 mM. In view that the solution with 20 mM salt concentration had a much lower protein concentration, this fact reinforces the role of the ionic strength in the protein surface adsorption process.

Molar absorptivity of bacteriochlorophyll *a* adsorbed onto different surfaces

The molar absorptivity of bacteriochlorophyll *a* adsorbed onto hydrophilic and hydrophobic surfaces from solutions with different ionic strengths were determined from eqn (1) across the measured spectral region using the results described in previous sections for absorbance, surface coverage, and sensitivity, and the results are presented in Fig. 9 and 10.

In the case of bacteriochlorophyll *a* adsorbed onto the hydrophilic peg silane surface, Fig. 9 shows that the increase in the ionic strength of the solution from 1 mM to 20 mM resulted in a significant narrowing of the Soret absorption band and an increase in its peak value by a factor of 1.3. As shown in Fig. 10, for the same range of salt concentrations, the molar absorptivity of surface-adsorbed bacteriochlorophyll *a* on the hydrophobic FDTS surface increased by a factor of 1.2 and we observe a broadening of the Soret peak.
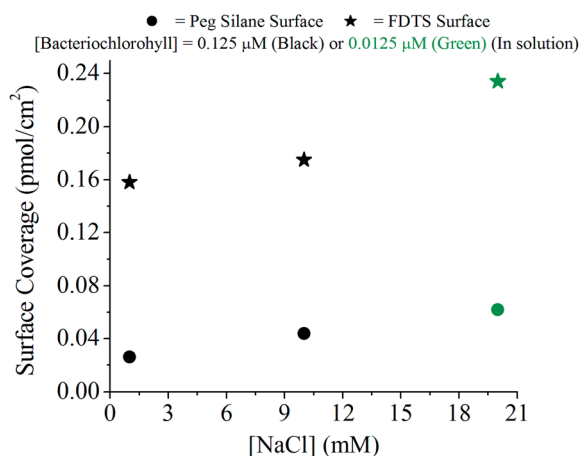

Fig. 8 Surface coverage measured for bacteriochlorophyll *a* adsorbed onto different surfaces that was previously dissolved in phosphate buffer solutions with different [NaCl]. It is worth noticing that 0.10 pmol cm^{-2} corresponds to an area of 41×41 nm^2 for each bacteriochlorophyll *a* molecule.
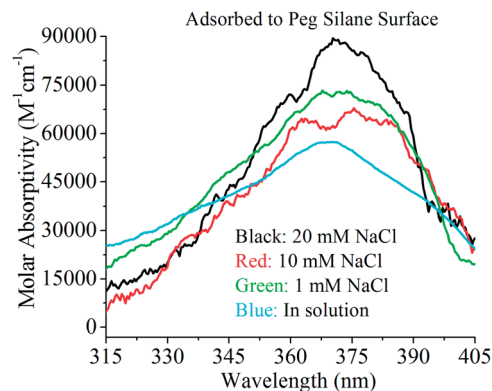

Fig. 9 Molar absorptivity measured for bacteriochlorophyll *a* adsorbed onto hydrophilic surface that was previously dissolved in phosphate buffer solutions with different [NaCl]. The light blue curve is the only exception that corresponds to the molar absorptivity calculated in solution.
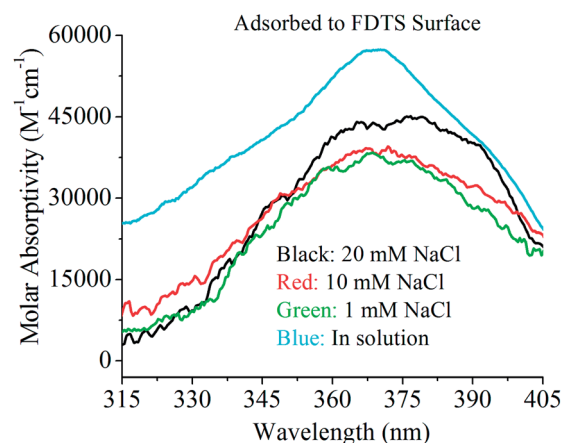

Fig. 10 Molar absorptivity measured for bacteriochlorophyll *a* adsorbed onto hydrophobic surface that was previously dissolved in phosphate buffer solutions with different [NaCl]. The light blue curve is the only exception that corresponds to the molar absorptivity calculated in solution.

It is important to notice that for bacteriochlorophyll *a* dissolved in solution under the same changes in ionic strength, there was no significant change in the molar absorptivity spectra, as already shown in Fig. 4. The molar absorptivity is the spectroscopic parameter that correlates with the molecular three-dimensional structure. It is well known to be dependent on the solvent composition when the molecules are dissolved in solution, and it has also been hypothesized that the adsorption process may affect the molecular structure due to unique surface interactions. In addition, it has been argued that the surface chemical composition can potentially impact those properties. The experimental results presented in Fig. 9 and 10 directly spectroscopically quantify those theoretical inferences.

The experimental results presented in this report show a strong correlation between the ionic strength of the phosphate buffer solution and both the spectroscopic characteristics of adsorbed bacteriochlorophyll *a* species and the amount of

adsorbed material. A possible explanation for the observed results is the aggregation of bacteriochlorophyll *a* due to the interaction with the surfaces of different compositions. As many of the current applications of this chromophore involve adsorption onto surfaces or interfaces,[48–50] these investigations can be particularly relevant.

Conclusions

We present here the development of a broadband single-mode integrated optical waveguide spectrometer for studies of surface-adsorbed species at sub-monolayer levels in the ultra-violet and visible spectral region. The combination of an aluminum oxide waveguide film (grown by an atomic layer deposition process) and a broadband grating coupler allowed us to experimentally acquire spectroscopic data down to 300 nm. To the best of our knowledge, this is the first time that broad-band spectroscopic data with an extremely sensitive single-mode IOW platform have reached this important spectral region. As an application of the developed tool, we described the impacts of surface functionalization on the physical properties of a specific chromophore using bacteriochlorophyll *a* as a probe material with its transition band centred at 370 nm. The extremely high sensitivity of the developed instrumentation enabled us to perform spectroscopic measurements for molecular films with surface densities in the femto moles per cm^2 range. The extension of the broadband single-mode integrated optical waveguide spectroscopy technique to the ultraviolet spectral region represents an important advance in studies of solid–liquid interfaces as a large number of biologically and chemically relevant species exhibits their transition bands in this part of the electromagnetic spectrum. The technology presented here can become instrumental to help elucidate several reaction mechanisms present at interfaces in nature and to enable new investigations of surface-confined species in thin-film technologies.

Acknowledgements

Notes and references

1 J. J. Ramsden, *J. Mol. Recognit.*, 1997, **10**, 109.
2 J. M. Brok and H. P. Urbach, *J. Mod. Opt.*, 2004, **51**, 2059.
3 F. Hook, J. Voros, M. Rodahl, R. Kurrat, P. Boni, J. J. Ramsden, M. Textor, N. D. Spencer, P. Tengvall, J. Gold and B. Kasemo, *Colloids Surf., B*, 2002, **24**, 155.
4 L. D. Shea, J. H. Jang, Z. Bengali and T. L. Houchin, *J. Biomed. Mater. Res., Part A*, 2006, **77**, 50.
5 D. Klee, D. Grafahrend, J. L. Calvet, K. Klinkhammer, J. Salber, P. D. Dalton and M. Moller, *Biotechnol. Bioeng.*, 2008, **101**, 609.
6 K. Miyabe and S. Takeuchi, *Anal. Chem.*, 1997, **69**, 2567.
7 G. Fleminger, G. Gertler and H. Rapaport, *Langmuir*, 2010, **26**, 6457.
8 G. Belfort and A. Sethuraman, *Biophys. J.*, 2005, **88**, 1322.
9 K. Nakanishi, T. Sakiyama and K. Imamura, *J. Biosci. Bioeng.*, 2001, **91**, 233.
10 B. Hofs, A. Brzozowska, A. de Keizer, W. Norde and M. A. C. Stuart, *J. Colloid Interface Sci.*, 2008, **325**, 309.
11 Y. Tie, C. Calonder and P. R. Van Tassel, *J. Colloid Interface Sci.*, 2003, **268**, 1.
12 M. Malmsten, A. L. Lindstrom and T. Warnheim, *J. Colloid Interface Sci.*, 1995, **173**, 297.
13 J. Homola, S. S. Yee and G. Gauglitz, *Sens. Actuators, B*, 1999, **54**, 3.
14 J. J. Ramsden, S. Y. Li, E. Heinzle and J. E. Prenosil, *Cytometry*, 1995, **19**, 97.
15 L. Heinrich, E. K. Mann, J. C. Voegel, G. J. M. Koper and P. Schaaf, *Langmuir*, 1996, **12**, 4857.
16 G. J. M. Koper and P. Schaaf, *Europhys. Lett.*, 1993, **22**, 543.
17 C. Kosslinger, E. Uttenthaler, S. Drost, F. Aberl, H. Wolf, G. Brink, A. Stanglmaier and E. Sackmann, *Sens. Actuators, B*, 1995, **24**, 107.
18 N. Saito and T. Matsuda, *Mater. Sci. Eng., C*, 1998, **6**, 261.
19 Z.-M. Qi, N. Matsuda, T. Yoshida, H. Asano, A. Takatsu and K. Kato, *Opt. Lett.*, 2002, **27**, 2001.
20 K. Kato, A. Takatsu and N. Matsuda, *Chem. Lett.*, 1999, **28**, 31.
21 I. Chabay, *Anal. Chem.*, 1982, **54**, A071.
22 P. W. Bohn, *TrAC, Trends Anal. Chem.*, 1987, **6**, 223.
23 K. Itoh and A. Fujishima, *J. Phys. Chem.*, 1988, **92**, 7043.
24 M. D. Degrandpre, L. W. Burgess, P. L. White and D. S. Goldman, *Anal. Chem.*, 1990, **62**, 2012.
25 D. S. Goldman, P. L. White and N. C. Anheier, *Appl. Opt.*, 1990, **29**, 4583.
26 S. S. Saavedra and W. M. Reichert, *Anal. Chem.*, 1990, **62**, 2251.
27 S. S. Saavedra and W. M. Reichert, *Langmuir*, 1991, **7**, 995.
28 K. Itoh and A. Fujishima, An application of optical waveguides to electrochemical and photoelectrochemical processes, in *Electrochemistry in Transition*, ed. O. J. Murphy, S. Srinivasan and B. E. Conway, Plenum, New York, 1992, p. 219.
29 C. Piraud, E. K. Mwarania, J. Yao, K. Odwyer, D. J. Schiffrin and J. S. Wilkinson, *J. Lightwave Technol.*, 1992, **10**, 693.
30 K. Kato, A. Takatsu, N. Matsuda, R. Azumi and M. Matsumoto, *Chem. Lett.*, 1995, 437.
31 S. B. Mendes, L. F. Li, J. J. Burke, J. E. Lee, D. R. Dunphy and S. S. Saavedra, *Langmuir*, 1996, **12**, 3374.
32 J. T. Bradshaw, S. B. Mendes and S. S. Saavedra, *Anal. Chem.*, 2002, **74**, 1751.
33 S. B. Mendes and S. S. Saavedra, *Appl. Opt.*, 2000, **39**, 612.
34 R. S. Wiederkehr, G. C. Hoops, M. M. Aslan, C. L. Byard and S. B. Mendes, *J. Phys. Chem. C*, 2009, **113**, 8306.
35 R. S. Wiederkehr, G. C. Hoops and S. B. Mendes, *Opt. Eng.*, 2011, **50**, 071109.

36 H. E. Ungnade and R. A. Smiley, *J. Org. Chem.*, 1956, **21**, 993.

37 W. T. Grubb and G. B. Kistiakowsky, *J. Am. Chem. Soc.*, 1950, **72**, 419.

38 Y. Inada, T. Saito, H. Ishikura, Y. Hada, K. Fukui, Y. Kodera and A. Matsushim, *Dyes Pigm.*, 2003, **56**, 203.

39 J. R. Lindsay Smith and M. Calvin, *J. Am. Chem. Soc.*, 1966, **88**, 4500.

40 M. M. Aslan, N. A. Webster, C. L. Byard, M. B. Pereira, C. M. Hayes, R. S. Wiederkehr and S. B. Mendes, *Thin Solid Films*, 2010, **518**, 4935.

41 M. B. Pereira, J. S. Craven and S. B. Mendes, *Opt. Eng.*, 2010, **49**, 124601.

42 C. M. Hayes, M. B. Pereira, B. C. Brangers, M. M. Aslan, R. S. Wiederkehr, S. B. Mendes and J. H. Lake, Sub-micron integrated grating couplers for singlemode planar optical waveguides, in *Proceedings of 17th IEEE University Governement Industry MicroNano Symposium (UGIM2008)*, IEEE - The Institute of Electrical and Electronic Engineers, Louisville KY USA, 2008, p. 227.

43 M. Wanebo, B. Kobrin, F. Helmrich and J. Chinn, Molecular vapor deposition (MVD™) - a new method of applying moisture barriers for packaging applications, in *International Symposium on Advantage Packaging Materials: Processes, Proprieties and Interfaces*, IEEE - The institute of Electrical and Electronic Engineers, March 2005, pp. 16–18.

44 B. Kobrin, T. Zhang, M. T. Grimes, K. Chong, M. Wanebo, J. Chinn and R. Nowak, *J. Phys.: Conf. Ser.*, 2006, **34**, 454.

45 A. F. Stalder, G. Kulik, D. Sage, L. Barbieri and P. Hoffmann, *Colloids Surf., A*, 2006, **286**, 92.

46 H. J. Permentier, K. A. Schmidt, M. Kobayashi, M. Akiyama, C. Hager-Braun, S. Neerken, M. Miller and J. Amesz, *Photosynth. Res.*, 2000, **64**, 27.

47 S. B. Mendes and S. S. Saavedra, *Opt. Express*, 1999, **4**, 449.

48 B. W. Henderson, A. B. Sumlin, B. L. Owcharrczak and T. J. Dougherty, *J. Photochem. Photobiol., B*, 1991, **10**, 303.

49 Y. Koyama, T. Miki, X.-F. Wang and H. Nagae, *Int. J. Mol. Sci.*, 2009, **10**, 4575.

50 J. C. Hindman, R. Kugel, A. Svirmickas and J. J. Katz, *Proc. Natl. Acad. Sci. U. S. A.*, 1977, **74**, 5.